DEVELOPMENT OF EQUIPMENT TO EVALUATE PRE-COLLISION SYSTEMS FOR PEDESTRIANS

Qiang Yi
Stanley Chien
Jason Brink
Yaobin Chen
Transportation Active Safety Institute, Indiana University-Purdue University Indianapolis
Rini Sherony
Toyota Motor Engineering & Manufacturing North America, Inc.
USA
Hiroyuki Takahashi
Toyota Motor Corporation
Japan

Paper Number: 13- 0221

ABSTRACT

Pre-Collision Systems (PCS) for avoidance/mitigation of pedestrian crashes have begun to be equipped on certain high-end passenger vehicles. At present, there is no common evaluation standard to evaluate and compare the performances of different PCS for pedestrian collision avoidance. The Transportation Active Safety Institute (TASI) at Indiana University-Purdue University-Indianapolis has been studying the establishment of such an evaluation standard with the support from Toyota Motor Corporation. To create a test environment for conducting PCS tests with pedestrians, common relative motion patterns of pedestrians and vehicles before crashes were identified. These motion patterns further define the requirements of the test equipment for PCS testing. The mannequin manipulation equipment was designed to provide sufficient motion range so that the mannequin motion can replicate pedestrian walking and running at the representative speeds. Various mannequin manipulation structures were considered and evaluated to ensure the safety and portability of the equipment and to minimize PCS sensing interference. Due to the potentially short intersection time period between the mannequin and vehicle in most test scenarios, the motions of the vehicle and the mannequin need to be precisely coordinated by a computer and must be based on sensor triggers. The final PCS test equipment design consists of a central computer, a mannequin with moving limbs, a crane system that can move the mannequin across or along the road, and infrared based start/stop sensors. Accurate data recording and the synchronization of mannequin motion and vehicle motion are based on the atomic clock in the Global Positioning System (GPS). This paper describes the design and development of the equipment for coordinating the relative motion of the mannequin and the test vehicle.

1. INTRODUCTION

Pre-Collision Systems (PCS) for pedestrian crash avoidance have been equipped on some high-end passenger vehicles. There are many studies on PCS pedestrian safety [1-4]. However, there is not a common evaluation standard to evaluate and compare the performances of PCS for pedestrian collision avoidance. The Transportation Active Safety Institute (TASI) at Indiana University-Purdue University-Indianapolis has been studying the establishment of such a standard with the support from Toyota Motor Corporation. One task surrounding the development of such a standard is the creation a set of test equipment for PCS pedestrian evaluation.

To create test equipment for conducting the PCS test with pedestrians, the possible types of relative motion between vehicles and pedestrians were identified. Then the representative motion speeds of vehicles and pedestrians were estimated. This information was used to generate the work space specifications of the mannequin manipulation equipment for vehicle testing. The wirelessly controlled mannequin manipulation equipment was designed to coordinate the operations of all system components for executing the PCS evaluation scenarios.

This paper is organized as follows: section 2 describes and analyzes the feasible test scenarios and speed ranges of the vehicle and the mannequin. Base on the result of section 2, section 3 gives an overall design of the mechanical structure of the system. Section 4 describes the computer network and control

structure of the whole test system. Section 5 demonstrates the experiment results. Section 6 concludes the paper.

2. EQUIPMENT REQUIREMENTS

To develop the equipment for PCS pedestrian collision avoidance evaluation, the most important task is to determine test scenarios which provide the specifications of the equipment. There are 12 types of common relative motion patterns between vehicles and pedestrians that can lead to crashes (see Table 1). For each type of relative motion patterns s, there is a set of tests to evaluate how PCS warning/braking are activated. The PCS performance is determined not only by how well it warns/brakes when there are imminent crashes but also how well it does not warn/brake when there are not imminent crashes (e.g., a pedestrian walks towards the street and stops at the curbside). Therefore, for each type of vehicle/pedestrian relative motion, there is also a set of tests to check if PCS does not activate when it should not activate. So there are a total of 24 types of test scenarios (see Table 1). Non-bold entries of Table 1 describe the motion directions of the mannequin.

The size of the mannequin workspace is determined by two factors. The first factor is the pedestrian motion speed and duration for all specified test scenarios. Literature suggested that the average pedestrian running speed is about 4.3m/s. Assuming that the mannequin needs to move at least 4.5 seconds during a PCS test along the road to give PCS sufficient time to detect the mannequin, the travel distance of the mannequin needs to be 19.35 meters long. However, travel speed of 4.3m across the road is too high for the PCS to respond to the imminent crash. First, the width of one lane road on highways is 3.7 m wide and many local streets are narrower. So it takes less than one second for the mannequin to cross the road. Second, most PCS systems take at least one second to recognize an imminent crash, to make the warning/braking decision and to command the brake system to engage the brake. Third, the PCS should not warn/brake if the pedestrian is not in the lane that the vehicle is moving. Therefore, the maximum cross road speed of the pedestrian is selected as 2.5m/s. Based on this selection, the width of the workspace of the mannequin motion device is calculated as 2.5x4.5 =11.25 m.

The second factor affecting the dimensions of the work space is the interference of the equipment to PCS radar signals. Considering two state of the art automotive radars used on the current PCS systems, the range of the vehicle radar elevations is 4.3°and 4.5°respectively. The range of the vehicle radar azimuth angles are 28° and 23°, respectively. The azimuth resolutions are ±2°and ± 1°, respectively. Assuming that the pedestrian detection range of the radar and video systems in the test vehicle is less than 40 m, when the vehicle is moving at 45 mph (72 km/h or 20 m/s), the pedestrian detected at 40 m away gives the vehicle 2 seconds to respond. The height of objects that the vehicle radar cannot detect at 40 m is 40m x tan(4.5^o) + 0.5 = 3.64 m (≈ 12 ft.). If the equipment can be kept above 3.64 m, the radar will not see the equipment within 2 sec. By the same calculation based on the azimuth resolution, the PCS radar should be able to tell that any object at 1.4 meter away from the road side is not an imminent crash threat. With the height of 3.64 m and width of 11.25 m, the RCS interference from the mannequin motion structure will not affect PCS's decision on warning/braking.

Table 1. Types of test scenarios

		Vehicle motion types					
		Straight		**Left turn**		**Right turn**	
Pede-strian motion types	**Crosses the road (PCS Activation)**	Cross from left to right	Cross from right to left	Cross from left to right	Cross from right to left	Cross from left to right	Cross from right to left
	Along the road(PCS Activation)	Away from the vehicle	Towards the vehicle	Away from the vehicle	Towards the vehicle	Away from the vehicle	Towards the vehicle
	Crosses the road (PCS non-Activation)	Move from left to right on curbside	Move from right to left on curbside	Move from left to right on curbside	Move from right to left on curbside	Move from left to right on curbside	Move from right to left on curbside
	Along the road (PCS non-Activation)	Away from the vehicle on curbside	Towards the vehicle on curbside	Away from the vehicle on curbside	Towards the vehicle on curbside	Away from the vehicle on curbside	Towards the vehicle on curbside

3. THE MECHANICAL STRUCTURE

3.1. The Selection of Mechanical Structures

Various mannequin motion devices were considered (see Figure 1), which include self-driven robot, jib crane, 2D bridge crane, 2D motion sled, on-ground track guided sled, and 1D gantry crane.

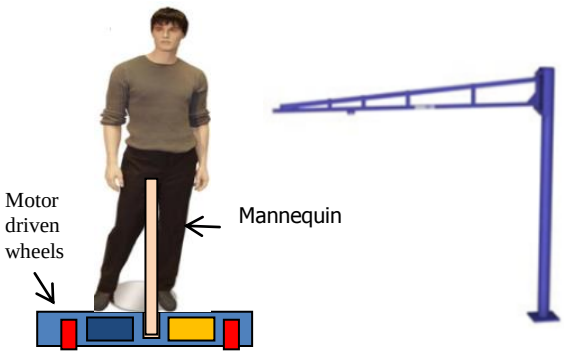

(a) Robot (b) Jib crane

(c) 2D bridge crane (d) Sled

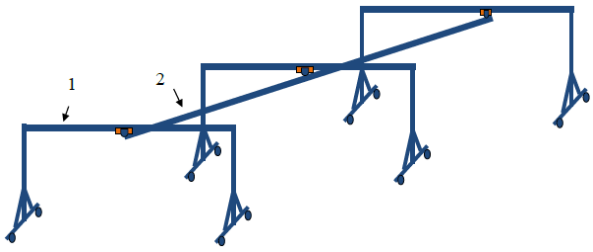

(e) 1-D gantry crane (1 = supporting beam, 2 = suspension beam)

Figure 1. Various mechanical structures considered for the manipulation of the mannequin motion.

The self-driven robot (Figure 1(a)) has many advantages, such as it has no work space size limitation, can produce 2-dimensional mannequin motion, and is very portable. However, it is not selected due to its following limitations, (1) the motion path may not be accurate due to road surface conditions, (2) the robot base needs to be at least 3 inches tall since the minimum motor diameter needs to be at least 2 inches for the torque needed for the robot motion, which may cause PCS false activation, (3) it can be damaged by the test vehicle and may damage the test vehicle if being run over by the test vehicle.

The jib crane (Figure 1(b)) can produce true 2-D mannequin motion but it is a large structure and requires a permanent installation at the test site. Also due to the concerns in the operation of a large jib crane, the jib crane is not selected for mannequin manipulation.

The 2D bridge crane (Figure 1(c)) also provides true 2D mannequin motion. It is stable with four standing poles and the track length can be extended along the road. However, it is not selected since the speeds of the commercially available gantry cranes are lower than 2.5 m/s and it needs to be permanently installed on the test site.

Sled (Figure 1(d)) approach for the mannequin motion manipulation was seriously considered due to its low radar interference, large workspace, and simplicity of the driving system. It can be driven by ropes or guiding track on the ground. When using rope to drive the sled, the operation of the sled and test vehicle is a concern since the rope can be tangled by the wheel of the vehicle. Since we do not own a test site, installing a mannequin guiding track below road surface is not an option to us.

We selected the 1D gantry crane system (Figure 1(e)) for the mannequin motion manipulation. This structure consists of several gantry cranes and a suspension I-beam hanging on multiple gantry cranes. The suspension I-beam can be extended as long as needed for pedestrian walking along the road scenarios by adding more gantry cranes. When testing pedestrian across road scenarios, the suspension I-beam can be pushed to one end of the gantry cranes and the mannequin can be moved along one gantry crane. When testing pedestrian moving along the road scenarios, the suspension I-beam can be moved to the middle of the gantry cranes and the mannequin can be moved along the suspension beam. This structure has several advantages: (1) the track length crossing the road can be over 11 meters and

the track length along the road can be extended as long as needed, (2) the mannequin can be moved crossing the road on the supporting I-beam and be moved along the road in suspending I-beam, (3) its overall weight is low and can be assembled and disassembled on the test site easily by 3-4 people. One drawback of this structure is that it cannot provide true 2-D mannequin motion. Since there is not sufficient data in crash databases to specify curved motion of pedestrians on the road, mechanical structure that supports one dimensional motion for crossing the road (with specified angle) and along the road is sufficient for the PCS evaluation.

3.2 Trolley and Harness

Once the 1-D gantry structure is selected, the rest of the mannequin motion manipulation system can be designed. The motion of the mannequin is controlled by a motor driven trolley (Figure 2) which runs on the I-beams of the crane structure. The connection of the trolley and the mannequin is through a harness (shown in Figure 3) which is attached to the bottom of the trolley. The harness consists of six main components, two lengthway support beams, two crossway support beams, two trolley connection beams, eight auto-lock fishing reels, sixteen guiding hooks and four strengthening steel plates. It has a dimension of 1825x2400mm, and weight of 10kg. Eight fishing lines are used to hang the mannequin. With the auto-lock fishing reels and guiding hooks, the height of the mannequin from ground can be adjusted. The harness is designed to reduce the swing and rotation of the mannequin caused by limb motion.

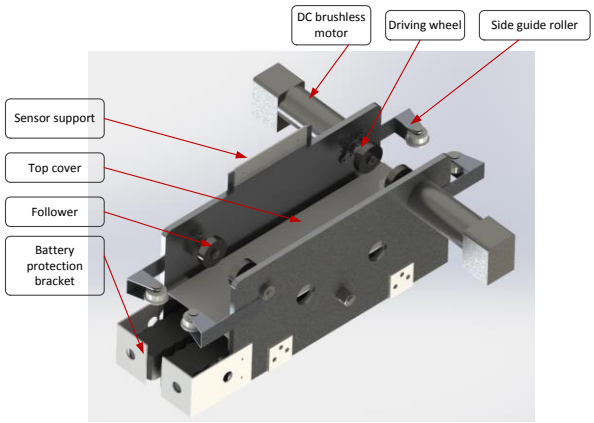

2(a)

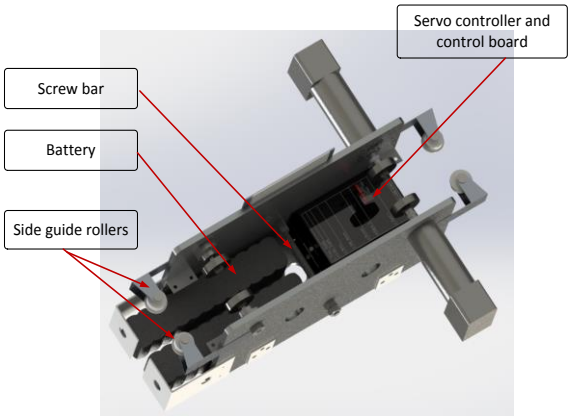

2(b)

Figure 2. The mechanical design of the trolley.

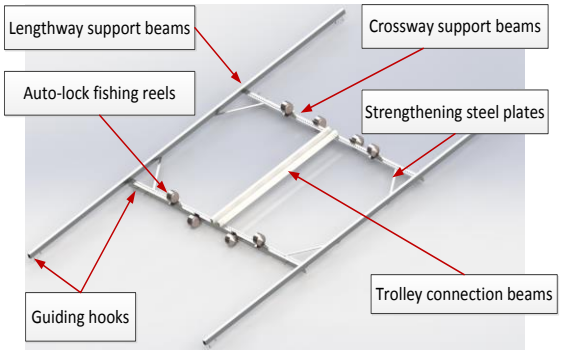

Figure 3. The structure of the harness.

4. COMPUTER CONTROLED SYSTEM OPERAION

4.1. Overview

To support the test of PCS for pedestrian crash scenarios, the operation of all system components need to be coordinated. The motion of the test vehicle, the motion of the trolley, and the motion of mannequin limbs need to be synchronized. The recordings of the test vehicle motion data and mannequin motion data also need to be synchronized. The system consists of a main control computer, two infrared based start and stop sensors, a trolley and a limb moving mannequin. Since the distances between different components are from several meters to hundreds of meters, all components operate on battery power and communicate wirelessly (see Figure 4). The mannequin can be driven by the trolley across the road or along the road.

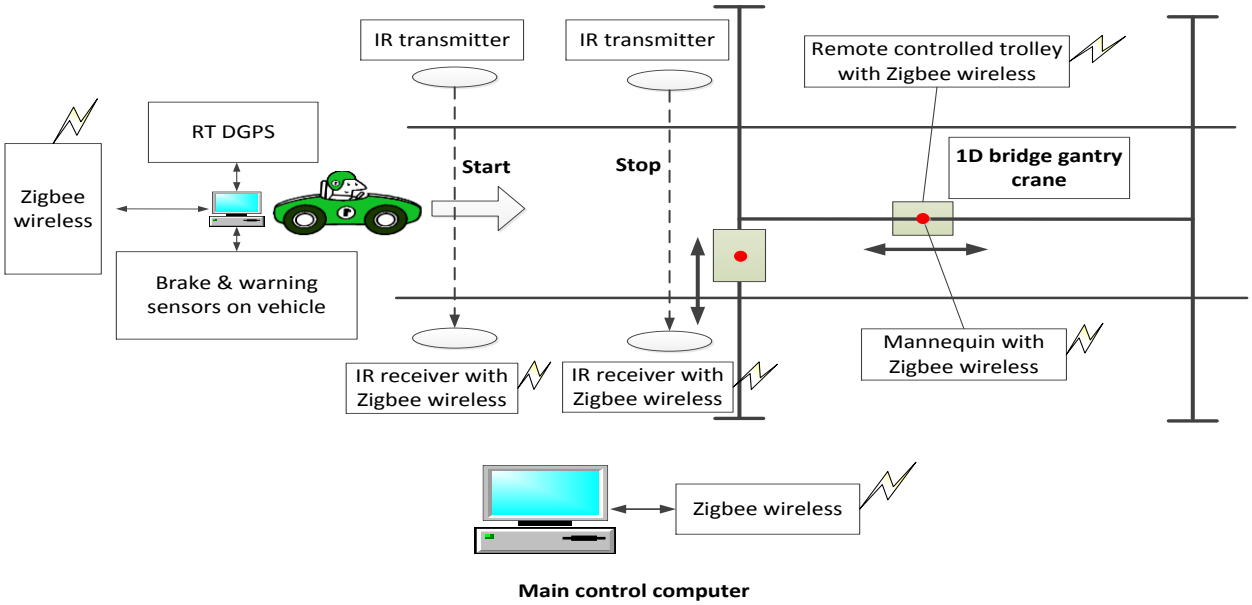

Figure 4. The overall design of the PCS evaluation system.

The main control computer is the core of the system. It coordinates the timed operation of all components in the system and interfaces with the operator. It also plans the motion timing of the mannequin and the trolley, coordinates data recording for the motion data of both the test vehicle and mannequin. The main control computer communicates with all other component devices through a Zigbee wireless communication network. Two long range infrared sensors (IR) are used to trigger the motion of the trolley and the mannequin based on the detection of the arriving test vehicle. One IR sensor detects the arrival of the test vehicle at a particular location and notifies the central computer wirelessly through a Zigbee network. The central computer then sends wireless messages to the trolley and the mannequin to start their pre-planned motion. The timing is calculated so that the vehicle and the mannequin meet at a predefined location. The other IR sensor detects the test vehicle at a distance of about 0.5 second to collision with the mannequin and notifies the mannequin wirelessly to cut off the power of all mannequin joint motors and the trolley in order to prevent motor damage due to overload during the crash. During the test, the trolley sends its GPS time stamped position and speed information to the main control computer periodically. The main control computer stores the time-stamped trolley position data and relays the data to the data recording computer inside the test vehicle. The data recording computer inside the test vehicle stores the combined the time stamped trolley motion data, the differential GPS measured vehicle motion data, and the time stamped various warning/braking signals for further analysis.

4.2. The Trolley Design

Due to the long span of the I-beams on the gantry cranes, the high trolley motion speed, and accuracy requirement, it is difficult to drive the trolley by a stationary motor through a chain or a rope. Therefore, a remote controlled and battery operated trolley is designed. The trolley contains two motors, motor servo drivers, an embedded microcontroller, a GPS timer, a Zigbee wireless communication module, limit sensors, and batteries. The connection block diagram of all components is shown in Figure 5.

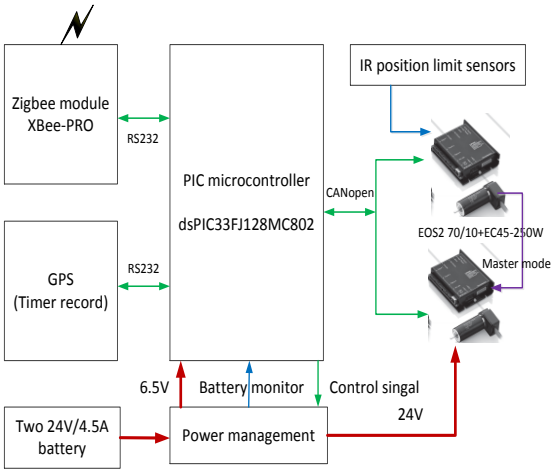

Figure 5. Control system of the trolley.

The embedded microcontroller communicates with the main control computer to get commands to control the motion of motors. The communication between the microcontroller and the main control computer is realized using a Zigbee module. The motor servo controller receives the motion commands from the embedded microcontroller and drives the motor using a PID controller. The communication protocol between the embedded microcontroller and the motor servo driver is CANopen protocol. To increase the load capacity and to reduce complexity of mechanical structure, we developed a direct drive system with two independent motors. Two 250 watts DC brushless motors are used. The motors are powered by two 24 Volt/4Ah NiMH rechargeable batteries. Each motor is controlled by a servo motor controller.

To ensure that two motors work synchronously, the motors are configured in such a way that one motor works in "Master Encoder Mode" and the other works in position or velocity mode. In this configuration, both motors follow the same reference input produced by a single external position encoder. The position encoder of the motors is also used to find the location of the trolley on the beam. To prevent accumulative position errors caused by wheel slip, the trolley controller recalibrates the location of the trolley after each round trip run using an infrared position sensor. The infrared sensor is also used as a safety limit sensor to indicate if the trolley is moving out of working range of the I-beam. A picture of the trolley prototype is shown in Figure 6.

Figure 6. Trolley prototype.

Due to the communication delay, it takes many milliseconds for the trolley position data to be sent to the main control computer for data recording. To ensure that the communication time delay does not cause data inaccuracy, the trolley position and speed data are time stamped by the embedded microcontroller before sending to the main control computer. The embedded microcontroller relies on a GPS timer module to provide the accurate wall clock time. The embedded microcontroller also supports self-diagnostic functions by reporting the heart beats and battery status to the main control computer periodically.

4.3. The Mannequin Design

To make the mannequin move like a real human, the mannequin with limb motion is designed. Motor driven joints are installed at the hips, knees and shoulders. Passive joints are installed at elbows which are driven indirectly by the motion of the upper arm.

The mannequin limb motion is realized by an electrical system that consists of a set of six servo motors, a motor controller, and an embedded microcontroller with a Zigbee networking module. A 7.4 v, 4200 mAh NiMH battery is used to drive the mannequin joints and the control system. The embedded microcontroller board monitors the battery charging levels and report to the main control computer periodically through the Zigbee network. Figure 7 is the connection diagram of the mannequin electrical circuit.

A PC controls the mannequin operation by sending mannequin motion commands to the embedded microcontroller in the mannequin through wireless Zigbee network. The embedded microcontroller passes the command (with desired position, speed and accelerations) to the motor controller which generates the proper PWM signals to all six servo motors according to the input commands.

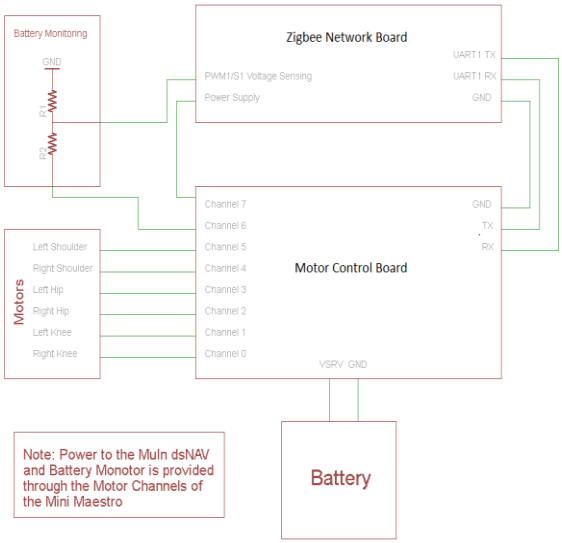

Figure 7. Control system of the mannequin.

Since PCS sensors detect pedestrians partially based on their body sizes and gestures, mannequins not only are built with heights and body sizes representative of the pedestrian public, but also should show major walking gestures. Many methods were proposed for biped robot walking gait planning based on mathematic planning method [5-8]. However, different from biped robots, mannequin's feet do not touch the ground, so that the mannequin limb motion does not require walking stability. Based on the published measured human gaiting data in the field of biomechanics, the gait functions of the hip and the knee in terms of speeds were generated in [12]. Figure 8 shows points and the fitted curve of one walking cycle at the speed of 1.2m/s. Figure 9 shows the stick frame of mannequin walking in one cycle (the sample interval is 100ms).

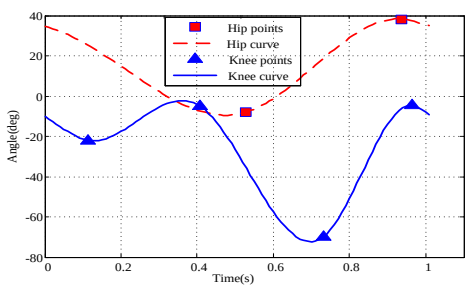

Figure 8. Angle points and fitted curve of mannequin's gait.

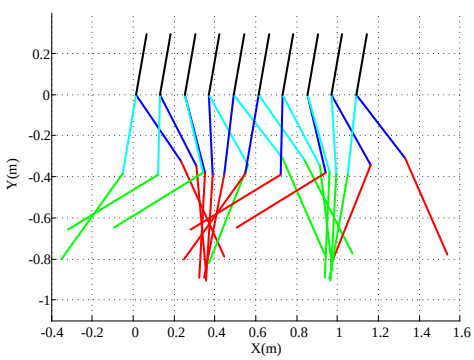

Figure 9. Stick frame of mannequin's one cycle walking.

5. EXPERIMENT

According to the system design as described in previous sections, a mannequin motion system prototype has been implemented. Figure 10 shows the demo of the successful coordinated motion of the trolley, harness and mannequin at the speed of 1.2m/s. Three pictures in the figure are the sequence of instances in one mannequin motion. Figure 11 shows the trolley's actual position and speed and the corresponding desired reference curves. It can be seen that position following is very accurate but the actual trolley speed has some fluctuations. This fluctuation is caused by torsional moment generated by mannequin motion.

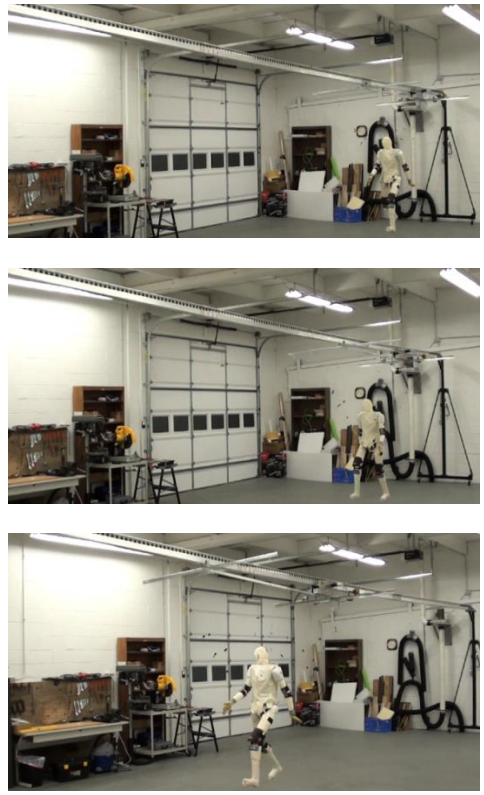

Figure 10. The trolley and mannequin motion at the speed of 1.2m/s.

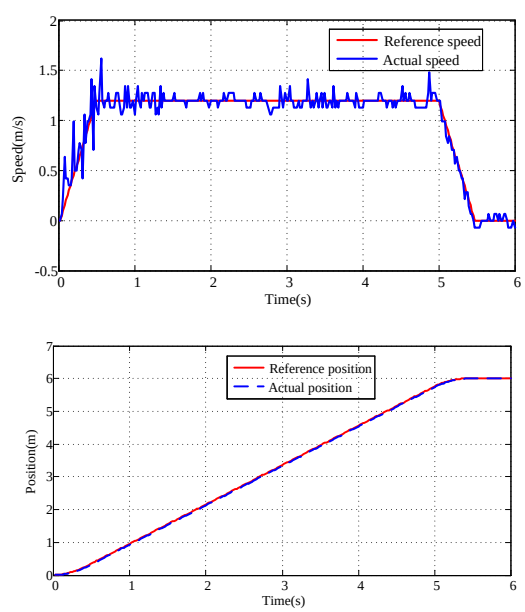

Figure 11. Speed and position following curves.

6. CONCLUSION

Based on PCS pedestrian test scenario types and the representative speeds of the vehicles and pedestrians, the mannequin motion equipment is designed. The equipment can cover the workspace of 11.4 m wide across the road and unlimited length along the road. It can be assembled and disassemble by 3-4 people manually. It is operated using a distributed computer control with the wireless Zigbee communication network. The vehicle and the mannequin motion data are time stamped based on GPS clock and stored synchronously. The whole system is battery operated. A prototype system has been built. The preliminary test was successful.

REFERENCES

[1] T. Gandhi, M. Trivedi, "Pedestrian protection systems: Issues, survey, and challenges" , IEEE Transaction on IEEE Transactions on Intelligent Transportation Systems, Volume 8, Number 3 (2011), 413–430, DOI:10.1109/TITS.2007.903444

[2] C. G. Keller, Thao Dang, H. Fritz, A. Joos, C. Rabe, D. M. Gavrila, "Active pedestrian safety by automatic braking and evasive steering" , IEEE Transactions on Intelligent Transportation Systems, Volume 12, Number 4 (2011), 1292-1304, DOI:10.1109/TITS.2011.2158424

[3] H.Kataoka, K.Tamura, Y. Aoki, Y. Matsui, "Extended CoHOG and particle filter by improved motion model for pedestrian active safety" , IECON 2012 - 38th Annual Conference on IEEE Industrial Electronics Society, (2012), 1511-1516, DOI:10.1109/IECON.2012.6388518

[4] S. Chien, Lingxi Li; Yaobin Chen, "A new braking and warning scoring system for vehicle forward collision imminent braking systems," ITSC 2012-15th International IEEE Conference on Intelligent Transportation Systems, (2012), 1103-1108, DOI:10.1109/ITSC.2012.6338775

[5] Q. Huang, K. Yokoi, S. Kajita, K. Kaneko, H. Arai, N. koyachi, K. Tanie, "planning walking patterns for a biped robot", IEEE Transaction on Robotics and Automation, Volume 17, Number 3, (2001), 280-289, DOI: 10.1109/70.938385

[6] G. Bessonnet, P. Seguin, P. Sardain, "A parametric optimization approach to walking pattern synthesis", International Journal of Robotics Research, Volume 24, Number 7, (2005), 523-536, DOI:10.1177/0278364905055377

[7] K. Harada, S. Hattori, H. Hirukawa, M. Morisawa, S. Kajita, E. Yoshida, "Two-Stage Time-Parameterized Gait Planning for Humanoid Robots", IEEE/ASME Transactions on Mechatronics, Volume 15, Number 5, (2010), 694-703, DOI: 10.1109/TMECH.2009.2032180

[8] F. Asano, M. Yamakita, N. Kamamichi, Zhi-Wei Luo, "A novel gait generation for biped walking robots based on mechanical energy constraint", IEEE Transactions on Robotics and Automation, Volume 20, Number 3, (2004), 565-573, DOI: 10.1109/TRA.2004.824685

[9] Robert L. Waters, Brenda Rae Lunsford, Jacqueline Perry, and Richard Byrd, "Energy- Speed Relationship of Walking: Standard Tables" Journal of Orthopedic Research, 6:215-222, Raven Press, Ltd., New York, 1988 Orthopedic Research Society, pp. 215-222. http://onlinelibrary.wiley.com/doi/10.1002/jor.1100060208/pdf

[10] Tommy Oberg, Alek Karsznia, Kurt Oberg, "Basic gait parameters: Reference data for normal subjects, 10-79 years of age," Journal of rehabilitation Research and Development Vol. 30 No. 2, 1993, pp. 210-223. http://www.rehab.research.va.gov/jour/93/30/2/pdf/oberg.pdf

[11] Tommy Oberg, Alek Karsznia, Kurt Oberg, "Joint angle parameters in gait: Reference data for normal subjects, 10-79 years of age," Journal of rehabilitation Research and Development Vol. 31 No. 1, August 1994, pp. 199-213. http://www.rehab.research.va.gov/jour/94/31/3/pdf/oberg.pdf

[12] Stanley Chien, Libo Dong, Qiang Yi, Yaobin Chen, Rini Sherony, and Hiroyuki Takahashi, "Joint Motion Pattern of Limb Moving Mannequins for Vehicle Active Safety Tests," ESV2013, Soul, Korea, May 2013.